MEDICAL ROBOTS

An ingestible self-propelling device for intestinal reanimation

Shriya S. Srinivasan[1,2,3]*, Julien Dosso[2], Hen-Wei Huang[1,2,3], George Selsing[1,2], Amro Alshareef[2,3], Johannes Kuosmanen[3], Keiko Ishida[2,3], Joshua Jenkins[3], Wiam Abdalla Mohammed Madani[2,3], Alison Hayward[2,3,4], Giovanni Traverso[1,2,3]*

Postoperative ileus (POI) is the leading cause of prolonged hospital stay after abdominal surgery and is characterized by a functional paralysis of the digestive tract, leading to symptoms such as constipation, vomiting, and functional obstruction. Current treatments are mainly supportive and inefficacious and yield acute side effects. Although electrical stimulation studies have demonstrated encouraging pacing and entraining of the intestinal slow waves, no devices exist today to enable targeted intestinal reanimation. Here, we developed an ingestible self-propelling device for intestinal reanimation (INSPIRE) capable of restoring peristalsis through luminal electrical stimulation. Optimizing mechanical, material, and electrical design parameters, we validated optimal deployment, intestinal electrical luminal contact, self-propelling capability, safety, and degradation of the device in ex vivo and in vivo swine models. We compared the INSPIRE's effect on motility in models of normal and depressed motility and chemically induced ileus. Intestinal contraction improved by 44% in anesthetized animals and up to 140% in chemically induced ileus cases. In addition, passage time decreased from, on average, 8.6 days in controls to 2.5 days with the INSPIRE device, demonstrating significant improvement in motility. Luminal electrical stimulation of the intestine via the INSPIRE efficaciously restored peristaltic activity. This noninvasive option offers a promising solution for the treatment of ileus and other motility disorders.

INTRODUCTION

Postoperative ileus (POI), affecting about 30% of patients undergoing surgery (1), represents the most prevalent cause of prolonged hospital stays (2). With an estimated economic burden exceeding $750 million in the United States (3), POI increases the cost of hospitalization by 71% on average (4, 5). Ileus is characterized by a functional paralysis of the intestinal tract, wherein a loss of peristaltic activity results in the symptoms of functional obstruction, gas and fluid accumulation, bloating, abdominal distension, constipation, vomiting, and nausea (6). Although commonly a complication of abdominal or pelvic surgery, other causes of ileus include infection, medications such as opiates (7), muscle dysfunction, and neural disorders (8). POI usually lasts between 2 and 6 days (9) and can manifest with gastrointestinal discomfort.

Current treatments are predominantly supportive in nature, including bowel resting, parenteral nutrition, prokinetic drugs, and, in severe cases, nasogastric tubing to relieve intragastric pressure (3). Nasogastric decompression not only is uncomfortable and requires hospitalization but also does not shorten the return of the first bowel movement and can result in procedure-related pneumonia. Drugs inhibiting sympathetic output and stimulating enteric cholinergic mechanisms have been investigated, although their utilization is limited by side effects. Early oral or nasoenteric postoperative feeding has been proposed, but their efficacy remains unclear (3). Similarly, the effects of gum chewing and pharmacological interventions are under investigation but currently inconclusive in results.

Electrical stimulation of the intestines to potentiate the enteric nervous system has been attempted in humans, although studies have not yielded consistent positive results (10–13). This stimulation was carried out through electrodes placed via a nasogastric tube targeting the gastric antrum and/or proximal small bowel (11). Many of these trials occurred in the 1970s with the limitations of placement, stimulation, and recording technologies of the time. However, more recent studies in animal models to stimulate the tract and to pace and entrain intestinal slow wave contractions via electrical stimulation show promising results (14, 15). Nevertheless, the use of nasogastric tubing and the placement of surface electrodes on the intestinal serosa for stimulation are impractical for clinical implementation. Further, these methods only target a small region of the intestines and would require ongoing hospitalization during the treatment period. As such, effective electrotherapeutic treatments for ileus await minimally invasive or ingestible devices that interface with the intestinal neuromusculature, withstand the cyclic deformation caused by peristaltic contraction, and perform stimulation along the length of the intestines to reactivate bowel transit.

Here, we describe the INSPIRE, an ingestible self-propelling device for intestinal reanimation, which electrically stimulates the intestinal enteric nervous system (ENS) to reanimate intestinal peristalsis (Fig. 1A). The device features an expandable design with electrode contacts on its outer surface to make stable contact with the lumen of the small intestine (SI), from which the ENS is located less than 1.5 mm (16) away (Fig. 1A). We hypothesize that this device can be safely ingested and will activate precisely in the SI upon contact with SI fluid on the basis of a pH-triggered expansion mechanism. Its mechanical properties will enable the device to expand within the intestine and make strong luminal contact with low impedance. It will then electrically stimulate the lumen, creating contractions that facilitate its strain-shifting form factor to propel the

[1]Department of Mechanical Engineering, Massachusetts Institute of Technology, Cambridge, MA 02139, USA. [2]Division of Gastroenterology, Hepatology and Endoscopy, Brigham and Women's Hospital, Harvard Medical School, Boston, MA 02115, USA. [3]David H. Koch Institute for Integrative Cancer Research, Massachusetts Institute of Technology, Cambridge, MA 02139, USA. [4]Division of Comparative Medicine, Massachusetts Institute of Technology, Cambridge, MA 02139, USA.
*Corresponding author. Email: shriya_srinivasan@fas.harvard.edu (S.S.S.); cgt20@mit.edu, ctraverso@bwh.harvard.edu (G.T.)
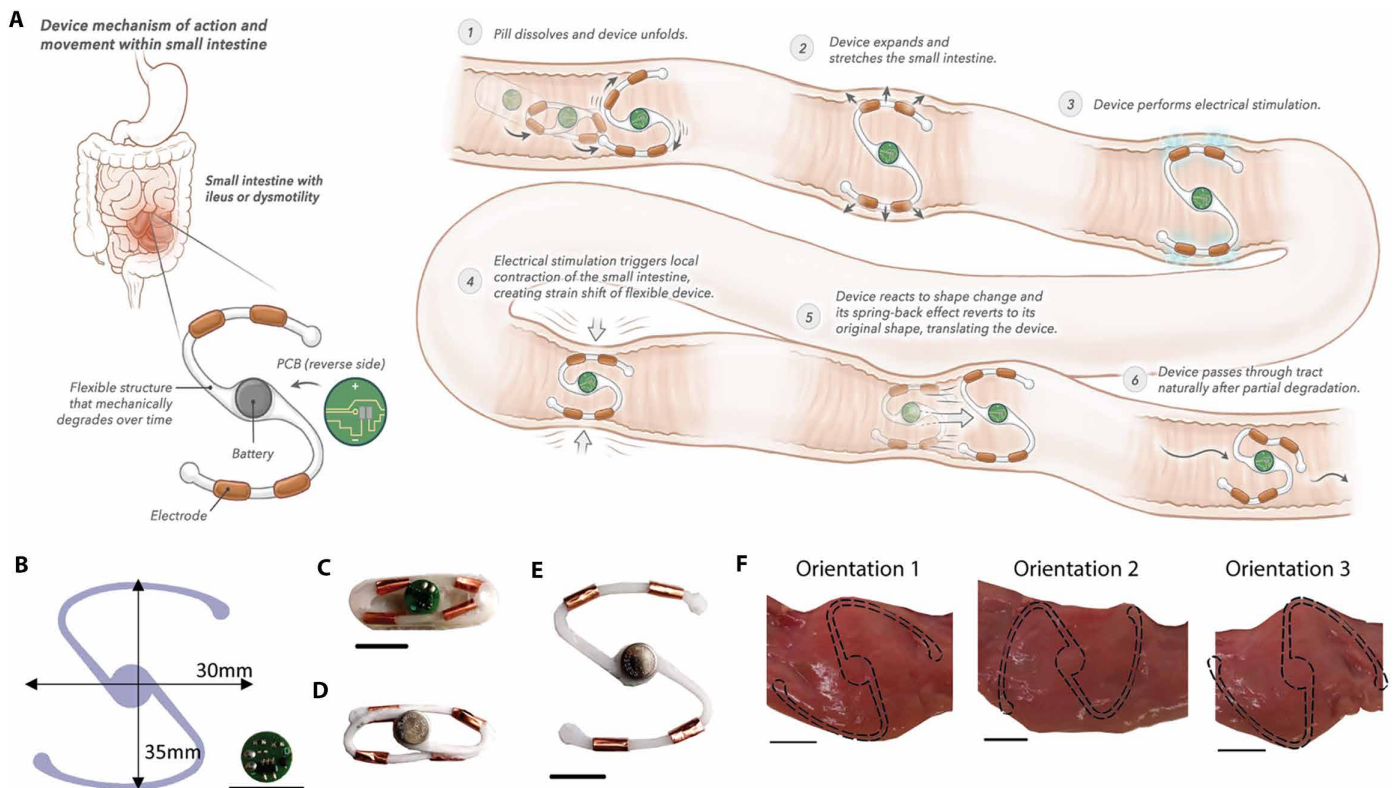
Fig. 1. Overview of the INSPIRE. (**A**) Mechanism of action of the INSPIRE for small intestinal motility. (**B**) INSPIRE form factor and geometry. (**C**) INSPIRE encapsulated in a triple-zero capsule with PCB in view. (**D**) Degraded INSPIRE after 2 hours of incubation in SIF. (**E**) Expanded INSPIRE with battery in view. (**F**) Three predominant orientations of the INSPIRE in small intestinal tissue, enabling luminal contact of electrodes. Scale bars, 10 mm.

translational movement of the device. The device will then degrade in less than 24 hours to enable safe passage and prevent any risk of tearing, perforation, or discomfort at the sphincters (Fig. 1A). We hypothesize that the device, by electrically stimulating the ENS and small intestinal musculature, will increase the motility rate in swine models of decreased motility.

RESULTS
INSPIRE design

The oral delivery method, need for functional activation, and autonomous passage requirements determined the overall form factor for the device. Oral ingestion dictated a maximal dimension commensurate with a triple zero capsule (closed length of 26.1 mm, an inner diameter of 9.55 mm, and a capacity of 1.37 ml), in which the device, electrical components, and battery were to reside.

To enable electrical stimulation, direct and sustained contact between the electrodes and the luminal mucosa of the SI is required, necessitating that the device could withstand and support the mass of the intestinal tissue above it. To prevent intestinal obstruction, the device must allow luminal contents to pass alongside itself and be able to move along the tract autonomously. Because segmental intestinal contractions yield bidirectional flow of chyme to enable fluid mixture and absorption, the device must also be able to move back and forth easily. The aforementioned functionalities must be viable in any orientation of the pill relative to the lumen. As such, an analysis of intestinal dimensions, folding properties, and pill geometries was

carried out to determine the primary shape of the INSPIRE (see Materials and Methods). Folds were prioritized along the longest dimension to leverage the oval shape of the capsule. Several three-dimensional (3D) and 2D designs were designed (Catia V5, Dassault Systèmes) and evaluated for the ease of fabrication, compressibility into a capsule, deformation, and ability to pass through a constrained pathway (fig. S1). Last, an S-shaped design was selected for optimization on the basis of its simplicity and performance in ex vivo simulations.

Geometry analysis to determine device shape

The unfolding event defined the minimum expanded device size, d—commensurate with the small intestinal diameter—necessary to stretch flaccid intestinal tissue and sustain mucosal contact from any possible orientation. Given a 2D cross-sectional contact frame, one possibility was a sphere of diameter d. Alternatively, a 2D structure will flatten from a cylindrical shape to a rectangular shape of the same surface area.

With no stretch in the vertical direction, because the surface area of the SI remains constant, the side length of this newly created rectangle sheet equals half of the SI's perimeter ($\pi d/2$). Consequently, a circle diameter $\pi d/2$ or greater was required. Below, we describe more detailed design processes and testing for each stage of the device's electromechanical performance.

Triggered activation

The device is designed to actuate through a pH-triggering mechanism upon contact with duodenal fluid at pH ≥ 5.5. To achieve

this, a triple zero gelatin pill was coated with Eudragit L 100-55 [poly(methacrylic acid-co-ethyl acrylate)] to achieve a 0.2- to 0.3-mm-thick coating. This polymer dissolves in the pH range present in the proximal to middle of the SI (Fig. 1A) (17). The accurate deployment of the device was assessed in vitro by placing the device in a bath of simulated intestinal fluid (SIF) at 37°C. The coating dissolved within 8.0 ± 3.2 min, and all devices were fully expanded under 10 min (n = 7 trials).

Expansion for luminal contact

The INSPIRE device was designed to make stable luminal contact to enable robust surface contact of the electrodes that would be positioned on the outside surface. The force required to luminally distend the SI 5 mm from its baseline was determined to be 0.1 N, using segments of freshly harvested swine SI (n = 3 ex vivo samples with n = 5 independent trials, Instron testing; see Materials and Methods). A safety factor of two was used to mechanically optimize the design by varying the thickness and material properties.

Static constraint simulations (Autodesk Fusion 360) were performed on each proposed design while holding forces constant and varying the polymer material options. Degradable polymers such as polycaprolactone (PCL) 37,000, polylactic acid (PLA), polyvinyl alcohol (PVA) 70,000, porcine gelatin, polyethylene oxide (PEO) 200,000, PEO 35,000, and (Soluplus, rice starch) were selected for their biocompatibility and degradation dynamics. Compression testing was performed on devices injection-molded from these polymers with diameters of 1.25, 1.5, and 1.75 mm. INSPIREs fabricated from a high-density polyethylene mixture of PCL (37,000) (35%) and PEO (200,000) (65%) demonstrated optimal compression and expansive properties at a thickness of 1.5 mm (fig. S2) because they balanced necessary rigidity with expansion force and expansion dimension. With this thickness, the device exerted 0.47 N against the wall of the pill. Upon expanding in the lumen, it exerted 0.22 N against the intestinal wall in orientation 1 (Fig. 1D), stretching the wall by an average of 5.5 mm (n = 7 trials). As Fig. 1F demonstrates, the device stretched the intestinal lumen independent of its orientation. In orientation 1, the device yielded a tissue strain of ~46%. Orientation 2 was the least favorable but still resulted in a tissue strain of 25%. Orientation 3 induced the most strain, up to ~48%. However, because the intestinal tissue can support strain up to 190% (18), these strains are safe. The mechanical forces induced on the wall may also aid in motility by stimulating subluminal stretch-sensitive mechanoreceptors. Further, the expansion of the lumen causes flattening of the intestine on one axis, thereby increasing the surface contact of the lumen to the surface of the INSPIRE to maximize electrical conductivity.

In benchtop tests, the INSPIRE devices were placed in freshly excised SI. In all three orientations, 20 ml of chyme collected from freshly harvest swine ileum were manually injected on the proximal side of the intestine at a rate of 1 ml/s, fully submerging the device in its surroundings. The fluid was able to flow past the device to the distal side and vice versa. This benchtop test ensures that the device geometry mitigates any obstruction to the bidirectional flow of chyme.

Mechanism of propulsion

Two modes of translation were taken into consideration for device propagation in the intestines: peristalsis and strain shift. Stretching of the intestinal lumen activates stretch mechanoreceptors in the

intestinal wall, which trigger reflexive peristaltic contractions (19). In the case of depressed or absent motility, electrical stimulation is expected to trigger axial muscular contractions. In both cases, muscular contractions yield unilateral deformation of the device, storing energy that the device automatically releases in a spring-back effect. The INSPIRE then localizes distally to an area with lesser mechanical resistance than the contracted ring, thus propagating in the tract.

Orientation and movement

The INSPIRE must operate independent of orientation and be capable of moving in both forward and backward directions to accommodate the bilateral movement that naturally occurs in the intestines to mix and propel food. We performed bench tests (n = 5 trials) to evaluate the orientation-independent excursion of the device and its ability to squeeze through curves or lumens of smaller diameter (10 mm), such as those that might be encountered in the turns of the small and large intestines (Materials and Methods and movies S1 and S2). In all cases, the device was able to pass without obstruction. The self-propelling ability of the device was evaluated by vertically compressing the device and measuring its horizontal displacement (movie S3).

Although the device has a self-propelling capability, its primary translation through the SI is expected to occur through peristalsis of the tract. Contractions of the tract will create an area of high mechanical resistance proximal to the INSPIRE and yield lateral translation in the distal direction. To ensure that reverse propagation or potential obstruction did not occur, we orally administered the INSPIRE to 10 swine and monitored the progression using x-ray and endoscopic monitoring every other day. In all 10 of 10 trials, no reverse propagation or obstruction was observed.

Cyclic deformation

Intestinal peristaltic waves occur at a frequency of 10 to 15 waves/min and can reach speeds of 1 to 4 mm/s (20). Cyclic testing, with conditions relevant to the intestinal peristalsis rate, was performed to ascertain the ability of the INSPIRE to withstand the cyclic peristaltic contractions of the intestines while maintaining its mechanical properties. After 30 min (600 cycles) and 60 min (1200 cycles) of sinusoidal activity, decreases in force of 3 ± 0.2% and 6 ± 0.3%, respectively, were observed due to the fatigue induced by plastic deformation (fig. S2). However, no signs of breaking were observed upon visual inspection for cracks, discoloration, and fractures, and the device was still able to expand to make luminal contact, demonstrating the durability of the device to withstand the intestinal contractions.

Degradation and passage

The polymers of the INSPIRE degrade with exposure to the basic pH of the intestine, weakening the mechanical strength of the device. Swine have passage times that range from 7 to 9 days (21). Hence, we designed a system that would degrade within 24 hours. We characterized the progression of degradation in solutions of pH ranging from 5.5 to 6.8, simulating the progression of the SI environment (Fig. 2E) (22). Device degradation was measured by performing compression testing, as described before and in Materials and Methods. Before each test, devices were dried using Kimwipes (KIMTECH, Kimberly-Clark) to eliminate moisture on the surface. At pH values of 5.5, 6.0, and 6.8, the device supports the intestinal tissue [F (intestinal distension force) > 0.1 N] for 3 hours, 2.75 hours,
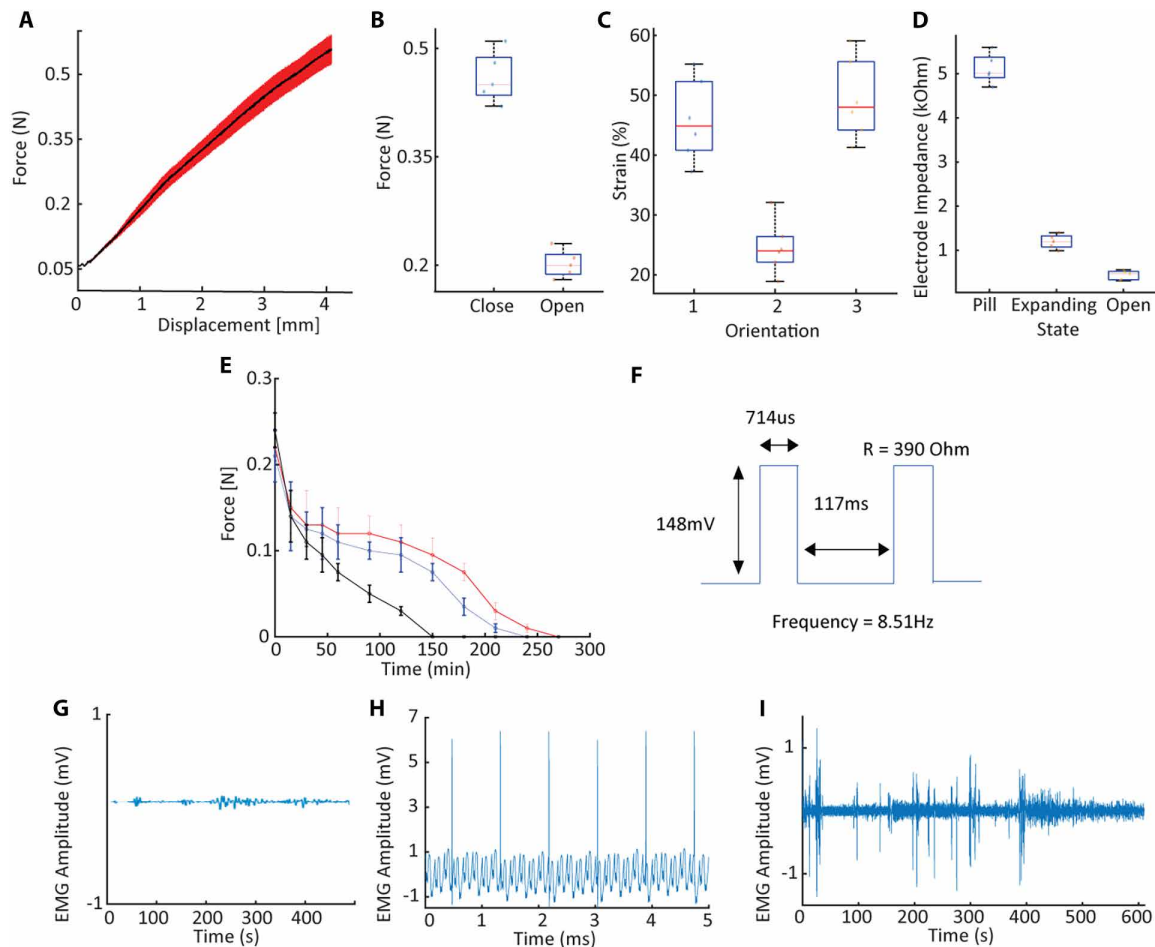
Fig. 2. Electromechanical properties of INSPIRE device. (**A**) Compression testing ($n = 3$ trials) of the device shows the capacity of the device to support intestinal weight (0.1 N) while deforming under intestinal contractions. (**B**) Forces exerted by the INSPIRE ($n = 5$ trials) in its closed configuration (9 mm) and open configuration (34 mm). (**C**) Intestinal tissue strain caused by the device expansion in its three primary orientations ($n = 6$). (**D**) Measured impedance of the electrodes ($n = 5$) inside the pill, in the expanding state, and once expanded inside the SI. (**E**) Measured force of the INSPIRE ($n = 3$) in a simulated intestinal environment with different pH 6.8 (black), 6.0 (blue), and 5.5 (red). The decrease of the force illustrates the degradation of the device. (**F**) Electrical stimulation pattern with a 1.5-V silver oxide battery and a 390-ohm resistor at the output. Representative electrophysiology from swine SI (**G**) under anesthesia, (**H**) during stimulation, and (**I**) electrical stimulation-induced muscle contractions.

and 50 min, respectively. After 4 hours, at any pH, the expansion force nears zero, facilitating unopposed passage in the colon and anorectal sphincter regions.

During the first 3 hours in the SI, the overall device geometry of the device remained largely unchanged because it degraded uniformly through surface erosion. A reduction of dimension of $57 \pm 5\%$ of the INSPIRE was measured, using digital calipers, over the course of 65 min. The location at which the arms bend degrades first, likely because of local defects induced by INSPIRE compression into a pill. The tips are secondarily affected, given their large surface area in contact with the intestinal fluid.

Optimizing electrodes, size, material, and placement

Having validated the mechanical properties of the device for ingestion, expansion, movement, degradation, and passage, we optimized the electrical properties to enable efficacious electrical stimulation. Strong mucosal contact and impedance were prioritized in the placement and size of the electrodes to facilitate efficient transmission of

current while minimizing power requirements. Given the S-shaped design, we opted to place four electrodes instead of two to increase the chance of contact amid the various orientations possible (Fig. 1F). Properties were characterized in freshly harvested swine SI with an intact mucus layer and used within 10 min of euthanasia. Ex vivo testing of electrode contacts at varying distances yielded a resistance of 14.5 ohm/mm (fig. S3A), wherein circuit resistance scaled with contact area by -20 ohm/mm^2 (fig. S3C). Four electrodes, each 10 mm^2, were positioned on either side of the device (Fig. 1, A and C) to maximize the chance of contact with the lumen. Electronics for stimulation control and the battery (1.55-V silver oxide) were housed in the central chamber of the INSPIRE, encapsulated with medical grade silicone (100 cSt; Liveo 360 Medical Fluid).

We designed a current-controlled stimulation program that delivers 1-mA pulses at 11 Hz (23), enabling consistent stimulation regardless of orientation as long as the tissue-electrode impedance is below 600 ohm. Electrode impedance of the device was measured to determine contact efficacy with the lumen ($n = 5$). While encapsulated in

the pill, expanding, and after making luminal contact, as visualized by endoscopic video, the impedance of the electrical contacts was 5.2 ± 0.19 megohm, 1.2 ± 0.18 kilohm, and 438 ± 0.12 ohm, respectively. Under these conditions, the INSPIRE's design and electronics enable delivery of up to 13.5 hours of continuous stimulation.

In vivo assessment of motility restoration
To evaluate the stimulating capabilities of the INSPIRE, electromyographic signals of intestinal electrical activity were recorded at baseline and with stimulation. Intestinal slow waves with a frequency of 0.25 Hz were observed at baseline (Fig. 2G). Stimulation delivered (11-Hz frequency) to the lumen was recorded by nearby electrodes (Fig. 2H) and elicited contractions from the musculature (Fig. 2I).

We then administered the INSPIRE to swine with unaltered (24–26) motility (control), anesthesia-induced dysmotility (27–32), and a model of ileus induced by intravenous glucagon (33–38) to determine effects on peristalsis and motility. Using high-resolution manometry (HRM), we characterized the motility at baseline and with stimulation (30-min segment for each). Representative examples of the motility pattern over a 10-min segment are showcased in Fig. 3 (A to D), corresponding to the contractions measured in the control and stimulated conditions. In the representative case, the root mean square velocity of the signal across all channels was 73% greater than that in the control condition, a significant increase ($P < 0.05$, two-tailed heteroscedastic t test). Across all unaltered swine, the contraction rate was significantly increased with INSPIRE-based stimulation from 0.025 contraction/s to 0.036 contraction/s (a 44% increase, $P = 0.005$, Student's two-tailed heteroscedastic t test, $n = 5$). Further, in a model of anesthesia-induced dysmotility, the contraction rate was significantly increased from 0.007 to 0.019 contraction/s (a 171% increase, $P = 0.2048$, Student's two-tailed heteroscedastic t test; Fig. 3E; $n = 6$). Moreover, in the model of induced ileus, the contraction rate was significantly increased from 0.015 to 0.036 contractions/s (a 140% increase, $P = 0.0207$, Student's two-tailed heteroscedastic t test). These demonstrate consistent increases in the peristaltic rate of the SI by the device regardless of the baseline neural activity state of the tissue. Contraction ratios between the stimulated and control conditions within each model further demonstrate that the INSPIRE has a significantly greater effect in the ileus model, where baseline neural activation is depressed (Fig. 3F). Movie S5 captures two instances of the device advancing in the SI after induced contractions.

Although INSPIRE-based stimulation of the SI evinced significant increases in intestinal contractions, motility is not necessarily correlated with contractile rate. Consequently, we measured the motility rate in swine by tracking passage time using a radiofrequency tracking pill (RFTP) codelivered with a sham pill (control group) or the INSPIRE (experimental group). For each animal, the RFTPs and shams or INSPIREs were endoscopically delivered to the duodenum to mitigate confounds associated with gastric motility or feeding status of the animal. The RFTPs reported the exact time of defecation. The average transit time in stimulated animals was significantly lower at 2.5 ± 1.2 (range 4) days as compared with 8.6 ± 2.9 (range = 8) days for controls ($P < 0.01$, one-tailed heteroscedastic t test; Fig. 4A).

Passage
A passage study of the device was conducted to ensure that the device could be easily excreted without discomfort at the sphincters

and anorectal region. INSPIRE devices were tracked using barium indicators visible with radiography during their course through the intestines (fig. S7). Radiography was performed using a ZooMax DIGI x-ray machine (Control-X Medical). Endoscopic assessment of the lumen after pill administration and passage demonstrated no overt adverse effects, including inflammation, perforation, infection, hematological complications, or abrasions ($n = 6$ animals). Further, through studies in terminal and survival settings, we know that the device does not impede gas and fluid movement, as observed during endoscopy and the lack of any obstructive side effects. Throughout all studies ($n > 20$ animals), veterinary staff and investigators did not observe any signs of discomfort or changes in behavior.

Biocompatibility
The selected polymers comprising the INSPIRE have established biocompatibility in humans. PEO (or PEG) is a biodegradable polymer that is US Food and Drug Administration (FDA) approved in many medical applications, such as laxatives (39) and drug delivery. PCL is a biodegradable polymer with low cell adhesion and has been FDA approved for applications including drug delivery (40) and suture (41). Toxicity studies, including those involving a combination of PCL and PEO, in rats have indicated no significant toxic effects (42, 43). Further, our device contains 9.8 mg of copper among all electronic components, which is below the tolerable upper intake levels for copper of 10 mg (44). In future prototypes, a more biocompatible metal will be used.

To further validate these properties and evaluate the encapsulation methods for the printed circuit board (PCB) and battery on board, we performed extract exposure tests on Caco2 cells in vitro using the extracts of the following substances incubated at room temperature for 7 days, unless otherwise noted: polymer degradation product, encapsulated battery and PCB as present in the device, INSPIRE incubated for 1 day, INSPIRE incubated for 5 days, an exposed battery and PCB to survey effects of a damaged INSPIRE, a toxin serving as a positive control, and saline as a negative control. After 3, 5, or 10 days of incubation with Caco2 cells, no significant differences were found among all experimental conditions, whereas the positive control significantly decreased cell viability ($P > 0.05$, one-tailed heteroscedastic t test; fig. S6). These results demonstrate that the polymer formulation does not present a significant safety risk and that the encapsulation of the electronics is sufficiently robust to withstand the intestinal environment.

Further, after treatment with INSPIRE and sham pill in in vivo studies, tissue sections were harvested, processed, and stained with hematoxylin and eosin. No differences were assessed between the control and treated tissues in terms of inflammation, mucosal integrity, and/or infection (Fig. 4, B and C).

DISCUSSION
Overall, this study demonstrates the design of an ingestible pill that expands and attains luminal contact to facilitate electrical stimulation of the ENS, inducing peristaltic contractions. In both models of normal intestinal motility and paralyzed ileus, stimulation significantly increased the local intestinal contractile rate and the overall motility of the intestines ($P < 0.05$). Last, after stimulation, the INSPIRE degrades and can be safely passed.

We anticipate that the INSPIRE could be either delivered orally or placed endoscopically in the intestines of patients after abdominal
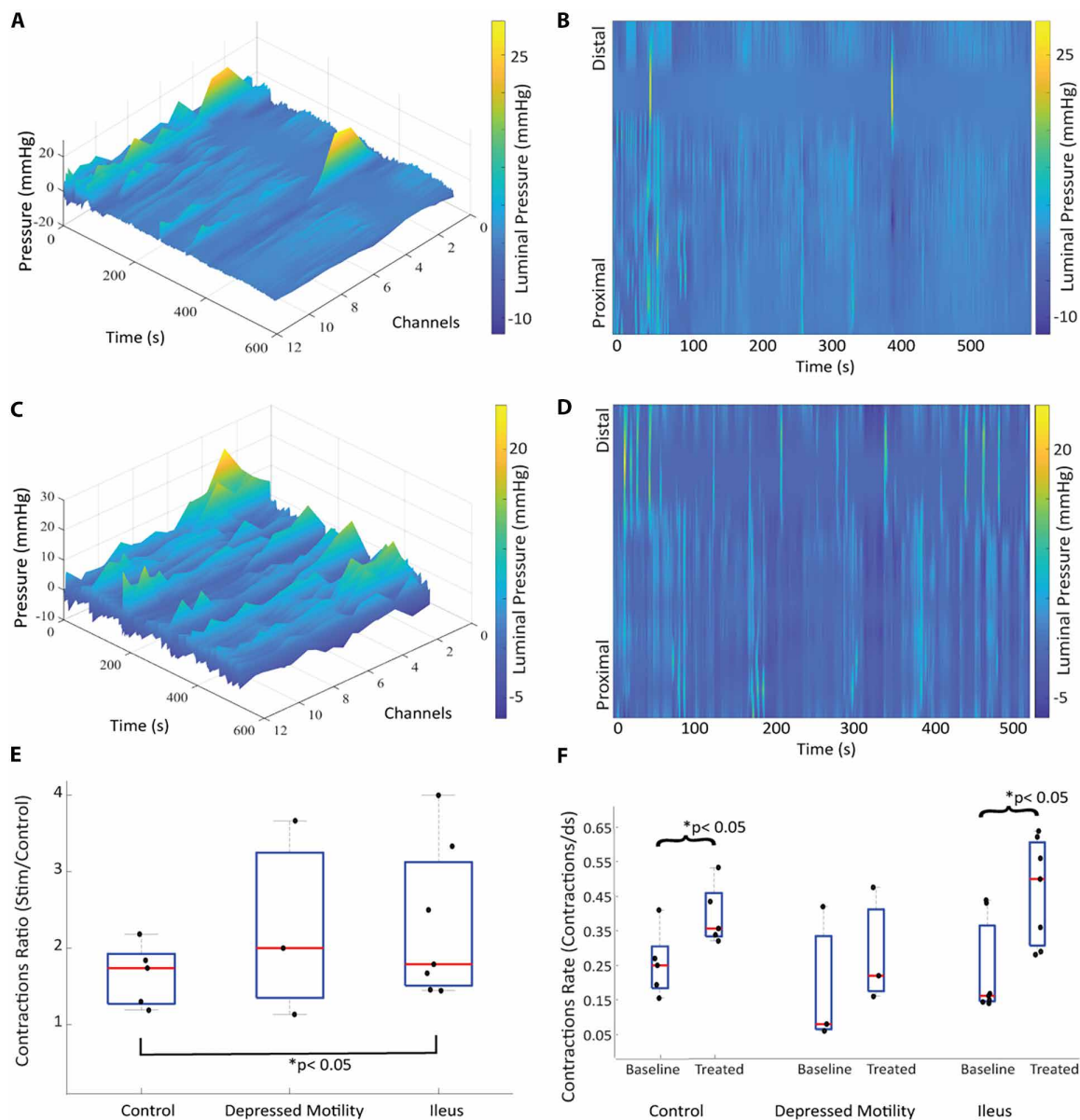
Fig. 3. In vivo effect on motility. Baseline intestinal luminal pressure by high-resolution manometry in (**A** and **B**) control and (**C** and **D**) stimulated conditions. (**E**) Contraction rate in control ($n = 5$), depressed motility ($n = 3$), and ileus ($n = 6$) models. (**F**) Contraction ratio control ($n = 5$), depressed motility ($n = 3$), and ileus ($n = 6$) models. The ratio is computed as the number of contractions during stimulation divided by that of the baseline. All ratios are higher than one, demonstrating an increased number of contractions due to the electrical stimulation.

surgery where POI is anticipated. Future studies will further establish the safety and efficacy and optimize electrical stimulation parameters to progress toward human translation. Dosing and concurrent administration of multiple devices must be evaluated. In addition, the effect of intestinal stimulation on changes of the intestinal microbiome should be investigated. On the basis of estimates of the material components and electronics at scale, we anticipate this device to scale cost-effectively. The material components of the INSPIRE are similar to those of FDA-approved ingestible devices, such as OROS capsules, ingestible temperature sensors, and capsule endoscopy systems, yielding comparable environmental considerations (*45*, *46*). Systems to

retrieve the electronic components from excreted waste must be considered to minimize the potential environmental complications of disposing electronic components into common sewage systems.

Components of this design, such as targeted delivery and luminal contact in the SI, may provide utility for related applications. For example, the expandable geometries may be used in devices that could autonomously collect luminal biopsies, deliver drugs directly into the mucosa, or stroke the mucosa to create parasthetic effects for diseases such as irritable bowel syndrome. The self-propelling property could be adapted for self-propelling endoscopy or colonoscopy capsules and applications requiring autonomous propulsion in
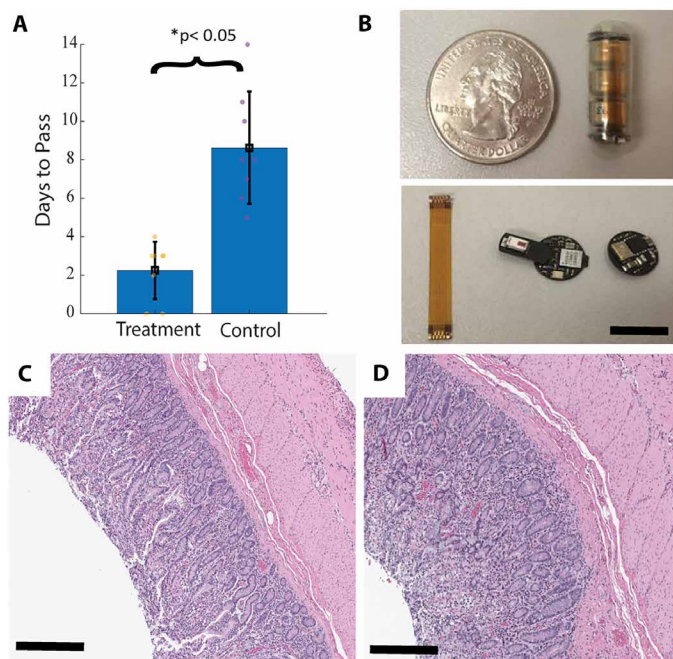
Fig. 4. Motility and biocompatibility. (**A**) The INSPIRE significantly decreased the number of days to pass through the tract, reflecting increased intestinal motility. (**B**) Motility rate was assayed by tracking passage time using an RFTP. Scale bar, 10 mm. Representative small intestinal tissue samples from (**C**) a control animal treated with a sham pill and (**D**) an animal treated with the INSPIRE demonstrate no significant difference. Scale bars, 1 mm (C and D).

tubular organs. Overall, this device will offer therapeutic options for POI and potentially other small intestinal conditions with neurological etiologies or involvement.

MATERIALS AND METHODS
Study design
Various designs for the INSPIRE were created, fabricated, and tested mechanically, as described below. In vitro and in vivo testing was then carried out to validate the functionality of the INSPIRE.

Geometry optimization
Three tests were performed to select the optimal geometry. The first test evaluated the residual deformation generated by encapsulation in the gelatin capsule. The 3D-printed prototypes made with the durable polyethylene resin of each design were measured with digital calipers before being housed for 24 hours in a triple-zero gelatin capsule. Then, each sample was removed from the gelatin pill, and dimensions were measured after 5 min to enable the device to fully expand. The second assessment characterized the ease of passage through constrained areas, mimicking the tortuous pathway of the intestines to minimize any risk of obstruction. Devices were placed in a lubricated tube of 25.4 mm in diameter 15 cm before a 2-cm section restricted to 10 mm in diameter. The prototype was attached to a strain gauge and manually pulled through the restricted section of the tubing at an attempted constant velocity of 0.6 mm/s. The maximal force to pass through the section was measured by the strain gauge (Nidec Shimpo, FG-3008). The final assessment evaluated the

self-propelling capability of each prototype. Inside lubricated tubing, prototypes underwent compressions of 10 mm by two opposing ball bearings. The horizontal displacement of the device in the tube was then tracked digitally using visual marker and recordings.

3D printing of devices
Initial prototypes for devices were designed and simulated using Autodesk Fusion 360 and printed using a Formlabs printer with durable high-density polyethylene resin. For custom polymer formulations, a negative mold was designed and 3D printed (Formlabs Form2) using the High Temp resin. Then, the polymer was heated to 145°C and injection-molded (S-100, Galomb Inc). Molds were sprayed with mold release (Universal Mold Release, Smooth-On) and preheated in an oven (Thermolyne Small Benchtop Muffle Furnaces, FB1415M) at 150°C for 1 hour. The device was left at ambient temperature for 30 min to cool down before opening the mold.

Compression testing
Devices were situated on a custom rig on the Instron 5943 Machine (Bluehill Universal, V4.28). The compression tests were done using a 2580-500 N static load cell in a displacement test setting with a fixed imposed rate of 0.2 mm/s rate over 5 mm and the rate of application kept free. The rate of compression and the outward force exerted by the device were analyzed. Before testing, devices were loaded into a triple-zero gelatin capsule (XPRS Nutra, NineLife) and were set in the constrained environment for at least 60 min to account for any potential plastic deformation induced by the constraint exerted by the pill. The device was placed between two compression plates (2501-085, Bluehill), with a custom rig consisting of two plates (2 cm by 2 cm by 1 cm) squeezing and holding in place the base of the device while ensuring free movement of the device. Cyclic compression testing was performed with 2000 cycles at a rate of 5 mm/s to mimic intestinal peristalsis and to ensure robustness of composition and detect weak points. These rates were picked to cover the maximal conditions of intestinal peristalsis, which can reach speeds of 1 to 4 mm/s.

Orientation and movement testing
A custom apparatus was assembled to simulate SI peristalsis. A flexible polyolefin plastic tube (McMaster) with a diameter of 25.4 mm, length of 30 cm, and wall thickness of 1 mm was used. The tubing was lubricated using mineral oil to mimic the luminal frictional properties of the SI. A restricted passage was made using two ball bearings (8-mm inner diameter, 22-mm outer diameter; McMaster) fixed 10 mm apart. The tubing was moved at a rate of around 0.6 mm/s by a stepper motor.

Ex vivo testing of device mechanics
To determine the strains imposed by the device's expansion, small intestinal tissue freshly harvested from swine within 10 min of euthanasia was placed in a petri dish and kept moist with Krebs buffer (Thermo Fisher Scientific) at 37°C. The circumference of the tissue was measured at baseline, after insertion of the device, and after removal of the device. Measurements were repeated three times for each possible orientation of the device. Each measurement was performed on an independent sample of tissue to prevent any confounds due to repeated deformation.

Further, devices were manually placed in all three orientations in the tissue sample. Then, 20 ml of chyme collected from freshly

harvest swine ileum was manually injected on the proximal side of the intestine at a rate of 1 ml/s using a large syringe feeding into the lumen, fully submerging the device in its surroundings. We then surveyed the distal side of the intestinal sample to observe whether the chyme was able to flow past the device without obstruction.

Luminal expansion testing
A 10-cm freshly harvest swine SI section was clamped on both sides longitudinally in its rested nominal size in the Instron. A traction test over 5 mm at a rate of 1 mm/s was performed to stretch the SI of 5 mm from its baseline, and the maximum measured force was recorded (Instron Bluehill).

Strain determination in ex vivo intestine
Two methods were used to measure SI strain: physical measurement of intestinal perimeter using digital calipers and quantification of photographs of the samples (ImageJ). Intestinal dimensions were measured pre- and post-device insertion in three orientations on different parts of the intestine from two swine.

Polymer formulation and dissolution assay
After optimization of the design using the durable 3D-printed resin, we transitioned to polymer formulation to fabricate the device out of degradable materials to enable easy passage. Mixtures of gelatin, PCL (37 kDa), and PEO (200 kDa) were mixed at 90°C using a mixer (Mix-Molder System M100, Galomb Inc.). Then, the polymer mixture was injection-molded at 90°C (benchtop injection molder S-100, Galomb Inc.) into a dog bone shape. Dog bone dimensions approximated the S curve dimensions with a length of 26 mm, a thickness of 1.5 mm, and a minimum width of 1.5 mm.

To offset the onset time of dissolution, devices were also dip-coated with Eudragit S100. Acetone (342.9 g), isopropanol (514.2 g), and water (42.9 g) were mixed. Then, 62.50 g of the Eudragit polymer was added to 50% of the diluent mixture and stirred for 60 min using a RCT basic IKAMAG at 200 rpm. At the same time, 6.25 g of triethyl citrate and 31.25 g of talc were added to the remaining diluent mixture and stirred for 10 min. The excipient suspension was then added to the Eudragit suspension, stirred for 5 min, then passed through a 0.5-mm sieve. Devices were dipped manually three times in the solution at 1-hour intervals and dried at room temperature. Each dipping added 30 mg ± 2 mg ($n = 5$) of coating.

SIF was prepared by mixing 6.8 g of potassium phosphate monobasic (Sigma–Aldrich) with 0.896 g of NaOH (Sigma–Aldrich) in 1 liter of distilled water. The pH was confirmed to be 6.8 using the Mettler Toledo FiveGo pH meter. Dog bones of each formulation were placed in tubes filled with 35 ml of SIF at 37°C and shaken at 50 rpm for 3 hours to simulate the intestinal movement present in the body. Dog bones were retrieved; gently dried with a paper towel; and photographed at 0, 15, 30, 45, 60, and 90 min each. Mechanical properties were assessed by folding each device in half and releasing. The spring-back force was measured using a tensile-testing machine (Instron, Bluehill).

Impedance testing
A 15-cm segment of SI, freshly harvested from swine, was sectioned longitudinally through a single incision, generating a rectangular tissue segment while keeping the mucus layer intact. Then, two electrodes at varying distances from one another (5, 10, 30, or 40 mm) measured circuit resistance and bipolar impedance using an LCR meter (Keysight E4980A/AL Precision) with a two-terminal setup at 100 kHz at 0.5 mA. Electrode surface area was optimized to balance contact area with the intestinal mucosa for stimulation while minimizing the overall impedance. Copper electrodes of varying sizes (10, 25, or 50 mm^2) were placed at a distance of 30 mm on the intestinal lumen because 30 mm corresponds to the maximal distance between electrodes on the expanded INSPIRE. Resistance and impedance were measured before placement, in SIF alone, and on the luminal surface ($n = 5$ trials).

Circuit design
A custom PCB was designed to output a frequency of 11 Hz, a high pulse width of 715 μs, and a pulse width of 120 ms, powered by a single 1.5-V silver oxide coin battery. Figure S8 provides a circuit schematic along with the details of the components used. A silver oxide 27-mAh battery (Digikey) with a capacity of 1.55 V, weight of 0.40 g, diameter of 6.8 mm, and height of 2.6 mm was selected for the INSPIRE. Taking into account the current consumption of 1 mA by the board and an additional 1 mA for the stimulation, the device can theoretically deliver 13.5 hours of continuous stimulation.

Animals and treatments
All animal surgeries were reviewed and approved by the Committee on Animal Care at the Massachusetts Institute of Technology (MIT) and adhered to Animal Research: Reporting of In Vivo Experiments (ARRIVE) guidelines and the NIH guide for the care and use of laboratory animals. Randomization was performed in the selected animals by blinding the operator with respect to whether stimulation was performed or not. All large animal studies were performed in a swine model (50- to 80-kg female Yorkshire swine). These were acquired from Cummings Veterinary School at Tufts University (Grafton, MA) ranging between 4 and 6 months of age. The swine model was chosen because its gastric anatomy is similar to that of humans and has been widely used in the evaluation of biomedical gastrointestinal devices (*47*). For survival studies, swine were anesthetized with an intramuscular injection of dexmedetomidine (0.03 mg/kg) and midazolam (0.25 mg/kg) and intubated and maintained on 2 to 3% isoflurane in oxygen. For terminal studies, pigs were sedated with an intramuscular (IM) injection of Telazol (tiletamine/zolazepam) and xylazine and given atropine via intramuscular injection. After intubation, anesthesia was maintained with isoflurane (1 to 3% in oxygen). Swine were fed Labdiet mini-pig grower pellets (5081) at 7:30 a.m. and 3:30 p.m. and a snack of fruit between 11 a.m. and 12 p.m. during studies. Endoscopy was performed in animals that were fasted overnight.

Three models were used to create conditions of dysmotility. In a survival experiment, anesthesia for less than 1 hour provided a 40 to 50% (*24, 26, 48*) reduction in motility. In terminal studies, anesthesia and deep sedation were used to induce a state of greater dysmotility (*30–32, 48*). Last, we created an animal model of ileus, wherein glucagon was intravenously injected at 10 to 14 mg per 50 kg of animal. On the basis of prior reports, this treatment results in a state commensurate with ileus where gastrointestinal transit is delayed by more than 50% (*14, 33, 37*).

At least 25 min of SI motility were captured at baseline and after induction for each case. To do so, an orogastric tube or overtube was placed with the guidance of a gastric endoscope and passed through the stomach into the SI. A high-resolution manometer (ManoScan 360, Medtronics) was inserted through the overtube to the SI and

recorded 25 min of baseline motility to assess the control condition. Then, encapsulated INSPIREs were placed into the SI. The correct deployment of the device was verified through endoscopic video, and the impedance of the electrodes was measured at 5-min intervals. Once the device was in place and correctly deployed, stimulation was initiated for 25 min, while the motility was recorded using manometry. During terminal experiments, a ventral midline laparotomy was performed to access the SI. A 0.5-cm incision was made in the intestinal wall to insert the device and manometer.

Electrophysiology
Electromyography signals were captured by placing electrodes on the SI close to the stimulation point and were measured using the Intan RHS 16-channel stimulation and recording controller (part #M4200) with a recording frequency of 10 kHz.

Motility assessment
A customized radio frequency (RF) tracking capsule comprising a Bluetooth low energy module 5.3 SoC (nRF52832, Nordicsemi) and a sensor (BME688, Bosch Sensortec) capable of sensing ambient temperature, pressure, and humidity was devised. The RFTP was encapsulated in a standard double-zero size capsule (outer diameter of 8.18 mm and overall closed length of 23.3 mm) together with epoxy (3M, DP100-CLEAR). The RFTP was composed of a Bluetooth SoC, thermistor, and batteries. The SoC with form factor of 5 mm by 5 mm integrates a Bluetooth module, Cortex-M4 with floating point unit (FPU), and antenna. The tracking was enabled by detecting the RF intensity attenuation by the tissue and the temperature, humidity, and barometric pressure variations to differentiate the capsule's location inside the animal body. An external RF station (nRF52 DK) was placed 1 m away from the animal near the housing to measure the RF intensity, reading the data from the sensor via Bluetooth. The temperature of RFTP inside the gastrointestinal tract was always above 38°C, and it dropped to room temperature (20°C) after excretion. All the PCBs were designed via Altium and manufactured via Bittele Electronics. The circuit schematic is provided as part of the Supplementary Materials. These RFTPs were administered to swine endoscopically in the SI along with a sham or operational INSPIRE pill at the same time. Transit times were then captured and compared between the treated and control groups.

Analysis of motility
The recorded HRM data were analyzed in MATLAB and processed through the following steps. Data were detrended to remove baseline drift occurring as a result of positional changes. Moreover, to remove the high-frequency artifact of respiratory rate (around a frequency of 0.5 Hz), a low-pass filter was applied. This low-pass filter does not overlap with the intestinal contraction rate of 10 to 14 contractions/min (0.2 Hz). Then, a peak detection algorithm was applied, with a minimum amplitude at 2 mmHg, area under the curve of 4 mmHg/s, and a minimum duration of 1.5 s. Visual inspection was used to confirm the peaks selected.

Passage study
Devices instrumented with radiopaque barium beads (BIPS, MediStore) were administered to the swine to determine the transit time and ensure safe passage of the devices. After administration of the device, swine were radiographed on day 0 and then on day 7. Using the barium trackers, progress and passage of the device were tracked.

Biocompatibility testing
We performed an extract exposure (49) test following ISO norms (10993-5) to evaluate the toxicity of the scaffold material. The following conditions were tested: the device (350 mg) [made of PEO (200 kDa; 66%) and PCL (37 kDa; 33%) in 30 ml of phosphate-buffered saline (PBS) (Thermo Fisher Scientific, J62036.K3], the device with uncoated silver oxide battery and PCB stimulator board in 30 ml of PBS, the device with polydimethylsiloxane (PDMS)–coated battery and stimulator board in 30 ml of PBS, and the device with PDMS only in 30 ml of PBS. The different samples were stirred at 37°C for 5 days, and 2 ml of solution was collected at 0.5-day intervals.

Moreover, different quantities of the polymer formulation (0.5, 1, or 2 g) were immersed in 20 ml of PBS and stirred at 37°C. Two milliliters of solution was collected after 7 days. Then, 100 μl of fetal bovine serum (Thermo Fisher Scientific, MFCD00132239) was added to each 900-μl aliquot of the samples and used to treat Caco2 cells (Koch Center for Integrative Research Repository) plated in a 96-well plate in triplicate. A negative control of untreated media and positive control of media containing MG-132 at a known concentration were also performed. At 24 and 72 hours, cell viability was measured through quantitation of adenosine 5′-triphosphate using CellTiter-Glo (Promega, USA) using a Tecan M1000Pro (Tecan Group, CHE).

Histological assessment of tissue
After euthanasia, the segment of intestine in which we placed the INSPIRE was harvested from each animal. All tissues were fixed in 4% paraformaldehyde, paraffin-processed, embedded, and then sectioned. Tissues were stained with hematotoxylin and eosin to study general structure and survey for potential trauma.

Statistical analyses
Quantitative data are reported as mean (±SD) or as a range when appropriate. The normality of the distributions was checked by the Shapiro-Wilk test. Comparative analyses were performed using Student's heteroscedastic two-tailed t test, unless otherwise noted. $P < 0.05$ was considered significant.

Supplementary Materials
This PDF file includes:
Figs. S1 to S8

Other Supplementary Material for this manuscript includes the following:
Movies S1 to S5
MDAR Reproducibility Checklist

REFERENCES AND NOTES
1. D. Wattchow, P. Heitmann, D. Smolilo, N. J. Spencer, D. Parker, T. Hibberd, S. S. J. Brookes, P. G. Dinning, M. Costa, Postoperative ileus—An ongoing conundrum. *Neurogastroenterol. Motil.* **33**, e14046 (2021).
2. E. P. Weledji, Perspectives on paralytic ileus. *Acute Med. Surg.* **7**, e573 (2020).
3. A. Luckey, E. Livingston, Y. Taché, Mechanisms and treatment of postoperative ileus. *Arch. Surg.* **138**, 206–214 (2003).
4. T. Asgeirsson, K. I. El-Badawi, A. Mahmood, J. Barletta, M. Luchtefeld, A. J. Senagore, Postoperative ileus: It costs more than you expect. *J. Am. Coll. Surg.* **210**, 228–231 (2010).
5. H. Mao, T. G. E. Milne, G. O'Grady, R. Vather, R. Edlin, I. Bissett, Prolonged postoperative ileus significantly increases the cost of inpatient stay for patients undergoing elective colorectal surgery: Results of a multivariate analysis of prospective data at a single institution. *Dis. Colon Rectum* **62**, 631–637 (2019).
6. N. Kaji, S. Nakayama, K. Horiguchi, S. Iino, H. Ozaki, M. Hori, Disruption of the pacemaker activity of interstitial cells of Cajal via nitric oxide contributes to postoperative ileus. *Neurogastroenterol. Motil.* **30**, e13334 (2018).

7. A. Kurz, D. I. Sessler, Opioid-induced bowel dysfunction: Pathophysiology and potential new therapies. *Drugs* **63**, 649–671 (2003).

8. A. Artinyan, J. W. Nunoo-Mensah, S. Balasubramaniam, J. Gauderman, R. Essani, C. Gonzalez-Ruiz, A. M. Kaiser, R. W. Beart, Prolonged postoperative ileus—definition, risk factors, and predictors after surgery. *World J. Surg.* **32**, 1495–1500 (2008).

9. C. R. Harnsberger, J. A. Maykel, K. Alavi, Postoperative Ileus. *Clin. Colon Rectal Surg.* **32**, 166–170 (2019).

10. J. A. Penfold, C. I. Wells, P. Du, I. P. Bissett, G. O'Grady, Electrical stimulation and recovery of gastrointestinal function following surgery: A systematic review. *Neuromodulation* **22**, 669–679 (2019).

11. A. M. Bilgutay, R. Wingrove, W. O. Griffen, R. C. Bonnabeau, C. W. Lillehei, Gastro-intestinal pacing a new concept in the treatment of ileus. *Ann. Surg.* **158**, 338–348 (1963).

12. D. C. Quast, A. C. Beall, M. E. Debakey, CLINICAL evaluation of the gastrointestinal pacer. *Surg. Gynecol. Obstet.* **120**, 35–37 (1965).

13. J. M. Moran, D. C. Nabseth, ELECTRICAL stimulation of the bowel. a controlled clinical study. *Arch. Surg.* **91**, 449–451 (1965).

14. J. Yin, J. D. Z. Chen, Mechanisms and potential applications of intestinal electrical stimulation. *Dig. Dis. Sci.* **55**, 1208–1220 (2010).

15. A. Abramson, D. Dellal, Y. L. Kong, J. Zhou, Y. Gao, J. Collins, S. Tamang, J. Wainer, R. McManus, A. Hayward, M. R. Frederiksen, J. J. Water, B. Jensen, N. Roxhed, R. Langer, G. Traverso, Ingestible transiently anchoring electronics for microstimulation and conductive signaling. *Sci. Adv.* **6**, eaaz0127 (2020).

16. P. Di Donato, D. Penninck, M. Pietra, M. Cipone, A. Diana, Ultrasonographic measurement of the relative thickness of intestinal wall layers in clinically healthy cats. *J. Feline Med. Surg.* **16**, 333–339 (2014).

17. M. Z. Khan, Z. Prebeg, N. Kurjaković, A pH-dependent colon targeted oral drug delivery system using methacrylic acid copolymers. I. Manipulation Of drug release using Eudragit L100-55 and Eudragit S100 combinations. *J. Control. Release* **58**, 215–222 (1999).

18. V. I. Egorov, I. V. Schastlivtsev, E. V. Prut, A. O. Baranov, R. A. Turusov, Mechanical properties of the human gastrointestinal tract. *J. Biomech.* **35**, 1417–1425 (2002).

19. M. Rao, M. D. Gershon, The bowel and beyond: The enteric nervous system in neurological disorders. *Nat. Rev. Gastroenterol. Hepatol.* **13**, 517–528 (2016).

20. R. K. Avvari, "Biomechanics of the Small Intestinal Contractions" in *Digestive System - Recent Advances* (IntechOpen, 2020); https://www.intechopen.com/chapters/67678.

21. L. J. Henze, N. J. Koehl, H. Bennett-Lenane, R. Holm, M. Grimm, F. Schneider, W. Weitschies, M. Koziolek, B. T. Griffin, Characterization of gastrointestinal transit and luminal conditions in pigs using a telemetric motility capsule. *Eur. J. Pharm. Sci.* **156**, 105627 (2021).

22. J. Fallingborg, Intraluminal pH of the human gastrointestinal tract. *Dan. Med. Bull.* **46**, 183–196 (1999).

23. K. B. Ramadi, S. S. Srinivasan, G. Traverso, Electroceuticals in the gastrointestinal tract. *Trends Pharmacol. Sci.* **41**, 960–976 (2020).

24. H. Chang, S. Li, Y. Li, H. Hu, B. Cheng, J. Miao, H. Gao, H. Ma, Y. Gao, Q. Wang, Effect of sedation with dexmedetomidine or propofol on gastrointestinal motility in lipopolysaccharide-induced endotoxemic mice. *BMC Anesthesiol.* **20**, 227 (2020).

25. T. Iirola, S. Vilo, R. Aantaa, M. Wendelin-Saarenhovi, P. J. Neuvonen, M. Scheinin, K. T. Olkkola, Dexmedetomidine inhibits gastric emptying and oro-caecal transit in healthy volunteers. *Br. J. Anaesth.* **106**, 522–527 (2011).

26. Y. Li, Y. Wang, H. Chang, B. Cheng, J. Miao, S. Li, H. Hu, L. Huang, Q. Wang, Inhibitory effects of dexmedetomidine and propofol on gastrointestinal tract motility involving impaired enteric Glia Ca2+ response in mice. *Neurochem. Res.* **46**, 1410–1422 (2021).

27. D. Noviana, A. Kandynesia, Reduction of intestinal motility and contractility in the cats anethized with Tiletamine-Zolazepam through contrast radiography study. *Jurnal Sain Veteriner* **30**, 10.22146/jsv.2621 (2012).

28. K. Nakamura, S. Hara, N. Tomizawa, The effects of medetomidine and xylazine on gastrointestinal motility and gastrin release in the dog. *J. Vet. Pharmacol. Ther.* **20**, 290–295 (1997).

29. S. Singh, W. N. McDonell, S. S. Young, D. H. Dyson, Cardiopulmonary and gastrointestinal motility effects of xylazine/ketamine-induced anesthesia in horses previously treated with glycopyrrolate. *Am. J. Vet. Res.* **57**, 1762–1770 (1996).

30. R. F. Quijano, N. Ohnishi, K. Umeda, F. Komada, S. Iwakawa, K. Okumura, Effect of atropine on gastrointestinal motility and the bioavailability of cyclosporine A in rats. *Drug Metab. Dispos.* **21**, 141–143 (1993).

31. H. Parkman, D. Trate, L. Knight, K. Brown, A. Maurer, R. Fisher, Cholinergic effects on human gastric motility. *Gut* **45**, 346–354 (1999).

32. T. J. Borody, E. M. M. Quigley, S. F. Phillips, M. Wienbeck, R. L. Tucker, A. Haddad, A. R. Zinsmeister, Effects of morphine and atropine on motility and transit in the human ileum. *Gastroenterology* **89**, 562–570 (1985).

33. Y. Nakatani, M. Maeda, M. Matsumura, R. Shimizu, N. Banba, Y. Aso, T. Yasu, H. Harasawa, Effect of GLP-1 receptor agonist on gastrointestinal tract motility and residue rates as evaluated by capsule endoscopy. *Diabetes Metab.* **43**, 430–437 (2017).

34. J. Xu, J. D. Z. Chen, Effects of cyclooxygenase-2 inhibitor on glucagon-induced delayed gastric emptying and gastric dysrhythmia in dogs. *Neurogastroenterol. Motil.* **19**, 144–151 (2007).

35. E. Mochiki, H. Suzuki, S. Takenoshita, Y. Nagamachi, H. Kuwano, A. Mizumoto, Z. Itoh, Mechanism of inhibitory effect of glucagon on gastrointestinal motility and cause of side effects of glucagon. *J. Gastroenterol.* **33**, 835–841 (1998).

36. H. Necheles, J. Sporn, L. Walker, Effect of glucagon on gastrointestinal motility. *Am. J. Gastroenterol.* **45**, 34–39 (1966).

37. G. K. Patel, G. E. Whalen, K. H. Soergel, W. C. Wu, R. C. Meade, Glucagon effects on the human small intestine. *Dig. Dis. Sci.* **24**, 501–508 (1979).

38. J.-L. Faillie, H. Yin, O. H. Y. Yu, A. Herrero, R. Altwegg, C. Renoux, L. Azoulay, Incretin-based drugs and risk of intestinal obstruction among patients with type 2 diabetes. *Clin. Pharmacol. Ther.* **111**, 272–282 (2022).

39. V. I. Smol'iakova, G. A. Chernysheva, M. B. Plotnikov, Laxative effect of poly(ethylene oxide) 1500 per se and in combination with bisacodyl. *Eksp. Klin. Farmakol.* **64**, 63–65 (2001).

40. T. Abudula, K. Gauthaman, A. Mostafavi, A. Alshahrie, N. Salah, P. Morganti, A. Chianese, A. Tamayol, A. Memic, Sustainable drug release from polycaprolactone coated chitin-lignin gel fibrous scaffolds. *Sci. Rep.* **10**, 20428 (2020).

41. N. Narayanan, L. Kuang, M. Del Ponte, C. Chain, M. Deng, "1 - Design and fabrication of nanocomposites for musculoskeletal tissue regeneration" in *Nanocomposites for Musculoskeletal Tissue Regeneration*, H. Liu, Ed. (Woodhead Publishing, 2016), pp. 3–29.

42. Z. Binkhathlan, W. Qamar, R. Ali, H. Kfoury, M. Alghonaim, Toxicity evaluation of methoxy poly(ethylene oxide)-block-poly(ε-caprolactone) polymeric micelles following multiple oral and intraperitoneal administration to rats. *Saudi Pharm J.* **25**, 944–953 (2017).

43. P. Grossen, D. Witzigmann, S. Sieber, J. Huwyler, PEG-PCL-based nanomedicines: A biodegradable drug delivery system and its application. *J. Control. Release* **260**, 46–60 (2017).

44. Office of Dietary Supplements, Copper; https://ods.od.nih.gov/factsheets/Copper-HealthProfessional/).

45. D. M. Bass, M. Prevo, D. S. Waxman, Gastrointestinal safety of an extended-release, nondeformable, oral dosage form (OROS®)1. *Drug Saf.* **25**, 1021–1033 (2002).

46. J. E. McKenzie, D. W. Osgood, Validation of a new telemetric core temperature monitor. *J. Therm. Biol.* **29**, 605–611 (2004).

47. K. Stamatopoulos, C. O'Farrell, M. Simmons, H. Batchelor, In vivo models to evaluate ingestible devices: Present status and current trends. *Adv. Drug Deliv. Rev.* **177**, 113915 (2021).

48. M. C. Torjman, J. I. Joseph, C. Munsick, M. Morishita, Z. Grunwald, Effects of Isoflurane on gastrointestinal motility after brief exposure in rats. *Int. J. Pharm.* **294**, 65–71 (2005).

49. G. K. Srivastava, M. L. Alonso-Alonso, I. Fernandez-Bueno, M. T. Garcia-Gutierrez, F. Rull, J. Medina, R. M. Coco, J. C. Pastor, Comparison between direct contact and extract exposure methods for PFO cytotoxicity evaluation. *Sci. Rep.* **8**, 1425 (2018).